COMPARISONS OF NONLINEAR TOROIDAL TURBULENCE SIMULATIONS WITH EXPERIMENT

W. DORLAND, M. KOTSCHENREUTHER, M.A. BEER[1],
G.W. HAMMETT[1], R.E. WALTZ[2], R.R. DOMINGUEZ[2],
P.M. VALANJU[3], W.H. MINER, Jr.[3], J.Q. DONG,
W. HORTON, F.L. WAELBROECK, T. TAJIMA, M.J. LeBRUN
Institute for Fusion Studies,
University of Texas at Austin,
Austin, Texas,
United States of America

Abstract

COMPARISONS OF NONLINEAR TOROIDAL TURBULENCE SIMULATIONS WITH EXPERIMENT.

The anomalously large thermal transport observed in tokamak experiments is the outstanding physics based obstacle in the path to a commercially viable fusion reactor. Although decades of experimental and theoretical work indicate that anomalous transport and collective instabilities in the gyrokinetic regime are linked, no widely accepted description of this transport exists so far. Here, detailed comparisons of first-principles gyrofluid and gyrokinetic simulations of tokamak microinstabilities with experimental data are presented. With no adjustable parameters, more than 50 TFTR L mode discharges have been simulated with encouraging success. Given the local plasma parameters and the temperatures at $r/a \simeq 0.8$, the simulations typically predict $T_i(r)$ and $T_e(r)$ within $\pm 25\%$ throughout the core and confinement zones. In these zones, the predicted thermal diffusivity increases robustly with minor radius. For parameters typical of $r/a > 0.8$, toroidal stability studies confirm the importance of impurity density gradients as a source of free energy potentially strong enough to explain the large edge thermal diffusivity, as first emphasized by Coppi and his coworkers. Advanced confinement discharges have also been simulated. The dramatic increase of $T_i(0)$ observed in supershots (from 5 to 30 keV) is recovered by our model for dozens of simulated experiments. Finally, simulations of VH and PEP mode-like plasmas show that velocity–shear stabilization of toroidal microinstabilities is quantitatively significant for realistic experimental parameters.

Introduction

Well-developed theoretical tools relevant to the description of anomalous transport (the gyrokinetic equation, the ballooning transform, collision operators, *etc.*) are readily available from the literature. However, numerical studies of anomalous transport that effectively utilize these tools

---

[1] Princeton Plasma Physics Laboratory, Princeton, New Jersey, USA.
[2] General Atomics, San Diego, California, USA.
[3] Fusion Research Center, University of Texas at Austin, Austin, Texas, USA.

for realistic parameters have until recently addressed only linear stability thresholds and quasilinear fluxes. Built upon existing theoretical foundations, recent advances in physics models[1, 2, 3, 4] have made numerical calculations of fully turbulent plasma processes more relevant and reliable. In this paper, we present detailed comparisons of first-principles simulations[1, 2, 3, 4, 5, 6, 7] of anomalous transport with experimental data. The general level of agreement found is very encouraging, especially since models of a few potentially important physical processes (e.g., non-adiabatic electrons, sheared flows, general geometry, impurity density gradients, etc.) remain to be fully integrated into the comparison study described here.

We first describe the simulation models that were employed in the present study, and then present our findings. Each of the gyrofluid and gyrokinetic codes used has been carefully benchmarked (linearly and nonlinearly, as appropriate) with related codes in the community, both as part of the US Numerical Tokamak Project and otherwise.

Gyrofluid Models

The nonlinear multispecies gyrofluid models utilized here describe wave-particle resonances[1], magnetic shear[2], FLR orbit-averaging[2], and toroidal drifts[3, 4], all in toroidal field-line-following coordinates[4, 3]. Non-linear gyrofluid trapped electron models and general-geometry coordinates have been developed,[4] but are not employed here. Sheared flows are included with either time-dependent ballooning transforms[5] or spatially varying equilibrium potentials[3].

The nonlinear simulations completed for this study typically have 2000–4000 independent modes (k_r, k_θ) on a 32–64 point field-line-following grid[3, 4]. The simulated volume is typically $63\rho_i \times 63\rho_i \times 6.3\,qR$ (i.e., $\sim 1.5\%$ of the total TFTR plasma volume), and the total simulated time is typically 50–100 growth times, or $250\,L_n/v_t \simeq 0.5\,msec$ for typical tokamak conditions. Larger-scale and longer-time simulations have been completed to demonstrate convergence[3, 4].

Gyrokinetic Models

A comprehensive linear electromagnetic $(\delta A_\parallel)$ gyrokinetic code that utilizes a unique implicit integration scheme has also been developed[6]. With fully gyrokinetic descriptions of four ion species and electrons (including trapped particle dynamics and a Lorentz collision operator), this balloon-

ing code calculates linear and quasilinear quantities in general geometry; the only significant approximations to the exact gyrokinetic dynamics are numerical, and can therefore be made arbitrarily small. Sheared flows are accounted for with a time-dependent ballooning transform. We also have a linear gyrokinetic integral eigenmode code[8] with which useful benchmarks and parameter scans have been completed.

TFTR L mode Confinement

Comprehensive linear gyrokinetic simulations of dozens of experimental profiles indicate that ion temperature gradient (ITG) driven modes are almost always the only linear instability present in the confinement zone ($r/a < 0.85$) of TFTR L mode discharges. Consequently, we focused first on distilling nonlinear ITG simulation results for χ_i as a function of a small number of relevant local plasma parameters into an approximate interpolation formula. The result is:

$$\chi_i\left(\{p_j\}\right) = C_0 \mathcal{F}\left(\{p_j\}\right) \mathcal{G}\left(\frac{R}{L_{T_i}} - \frac{R}{L_{T_i\text{crit}}(\{p_j\})}\right) \frac{\rho_i^2 v_{ti}}{R} \qquad (1)$$

in which $C_0 = 14$ and $\mathcal{G}(x) \equiv \min\left(x, x^{1/2}\right) H(x)$. Here, $H(x)$ is a Heaviside function. The notation $\{p_j\}$ indicates the set of local plasma parameters, and

$$\mathcal{F}\left(\{p_j\}\right) = \frac{q}{2 + \hat{s}}(1 - n_b/n_e)(1 + \epsilon/3)\frac{f(Z^*_\text{eff}, \tau)}{\tau}$$

$$f = \begin{cases} 1 + 0.1/\tau & Z^*_\text{eff} \leq 3 \\ 2(3.5 - Z^*_\text{eff}) + 0.1/\tau & 3 < Z^*_\text{eff} \leq 3.5 \\ 0.2(Z^*_\text{eff} - 3.5)/\tau + 0.1/\tau & 3.5 < Z^*_\text{eff} \end{cases}$$

The critical ion temperature gradient is approximately

$$\frac{R}{L_{T_i\text{crit}}} = 2.8\sqrt{1/2 + 1/q}\; G\left(\{p_j\}\right)\left(1 - 0.85\epsilon/\hat{s}^{1/4}\right) \qquad (2)$$

$$G\left(\{p_j\}\right) = g(\{p_j\})\, h(\hat{s}, R/L_n)$$

$$g = \max\left[0.57, g_1(Z^*_\text{eff})\right]\left(\frac{\tau}{1 - n_b/n_e}\right)^{g_2(Z^*_\text{eff})}$$

$$g_1 = 1.26 + |Z^*_\text{eff} - 3|\left(-0.27 + 0.075\, Z^*_\text{eff} - 0.044\, Z^{*2}_\text{eff}\right)$$

$$g_2(Z^*_\text{eff}) = 0.61 - \frac{0.27}{1 + \exp\left\{8(3.3 - Z^*_\text{eff})\right\}}$$

and

$$h = |0.1976 - 0.4550\,\hat{s} + 0.1616\,R/L_n|^{0.769} + 0.7813 + 0.2762\,\hat{s} + 0.3967\,\hat{s}^2.$$

The temperature ratio $\tau \equiv T_i/T_e$, the hot ion (beam) density is n_b, and

$$Z_{\text{eff}}^* \equiv \frac{Z_{\text{eff}} - n_b/n_e}{1 - n_b/n_e}$$

upon assuming carbon is the only impurity and that the hot ions are hydrogenic. The remainder of the notation is standard.

Eq. (1) was found with the nonlinear gyrofluid codes. Eq. (2) was found with the implicit linear gyrokinetic code. Qualitatively, Eqs. (1) and (2) are unsurprising; stabilizing trends for ITG modes from $\hat{s}$, T_i/T_e, Z_{eff}, $q^{-1} \propto I_p$, and R/L_n are familiar from the literature. Several simplifying assumptions (generally consistent with TFTR L mode transport) were used in deriving Eqs. (1) and (2), including adiabatic electrons, $\beta = 0$, circular flux surfaces, and zero velocity (and diamagnetic) shear. Significant dependences of $\mathcal{F}$ and $L_{T\text{crit}}$ on velocity shear, the carbon density gradient, non-carbon impurities, *etc.* are not included in these interpolation formulae. For the moderate collisionalities typical of TFTR L modes, we find that including the proper non-adiabatic electron response typically doubles the growth rate[3] without significantly affecting $L_{T\text{crit}}$ or the quasilinear ratio of χ_i/χ_e; the simplest estimate of this effect based on linear and preliminary nonlinear simulations[4] would therefore be to double C_0. Interestingly, changes to C_0 and $\mathcal{F}$ are of less consequence than one might have initially guessed. In the collisionless regime, trapped electron modes can significantly affect $L_{T\text{crit}}$, and are therefore potentially more important.

Sensitivity. The gyro-Bohm form of Eq. (1) implies that the local temperature is relatively insensitive to C_0. In steady state, the power deposited inside a flux surface must equal the heat flux through that surface; for a gyro-Bohm process, this implies $P_{\text{dep}} \propto C_0 T^{5/2}$. As a result, $T \propto (C_0/P_{\text{dep}})^{-2/5}$. Moreover, for typical profiles, $C_0 T^{3/2}$ is large enough in the center of the discharge to enforce marginality. Our profile simulations indicate that, together, these effects typically result in $T_0 \propto C_0^{-1/4}$. The central temperature is usually much more sensitive to variations in $L_{T\text{crit}}$. Fortunately, this is a linear parameter that can be more reliably calculated.

Criticality. We emphasize that Eqs. (1) and (2) are theoretically derived results from numerical toroidal simulations; no features of this model
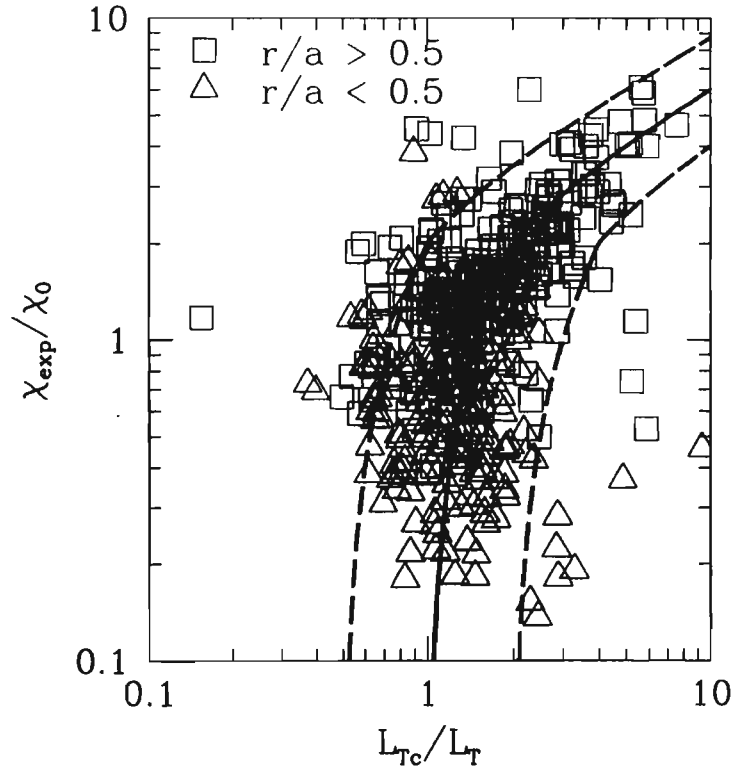
FIG. 1. *Comparison of theory with experimental TFTR data taken from the MFE database.*

were obtained by referring to experimental data. Our estimate for the ion thermal diffusivity can be written as the product of a parameter-dependent coefficient and a function of the deviation of the temperature gradient from marginality; $\chi_i = \chi_0 \hat{\mathcal{G}}(L_{T\text{crit}}/L_T - 1)$. In Fig. (1) we compare this estimate with experimental data taken from the Magnetic Fusion Energy Database. Eleven radial points $(0.3 < r/a < 0.7)$ from each of fifty-four TFTR discharges (all post-1988 MFEDB shots from TFTR) are included. The solid line represents the theoretical expectation; the dashed lines indicate variations in L_T of factors of 2, our rough estimate of experimental uncertainty. When χ_0 is large compared to the experimentally inferred χ, one expects and finds that $L_T \sim L_{T\text{crit}}$. For $r/a > 0.5$, χ_0 falls with the decreasing temperature and the departure from marginality is pronounced. Our theoretical estimate of the thermal diffusivity encompasses both regimes.

Power Balance Calculation

We have used Eqs. (1) and (2) in two independent steady-state power balance codes that predict the temperature profiles with comparable results.
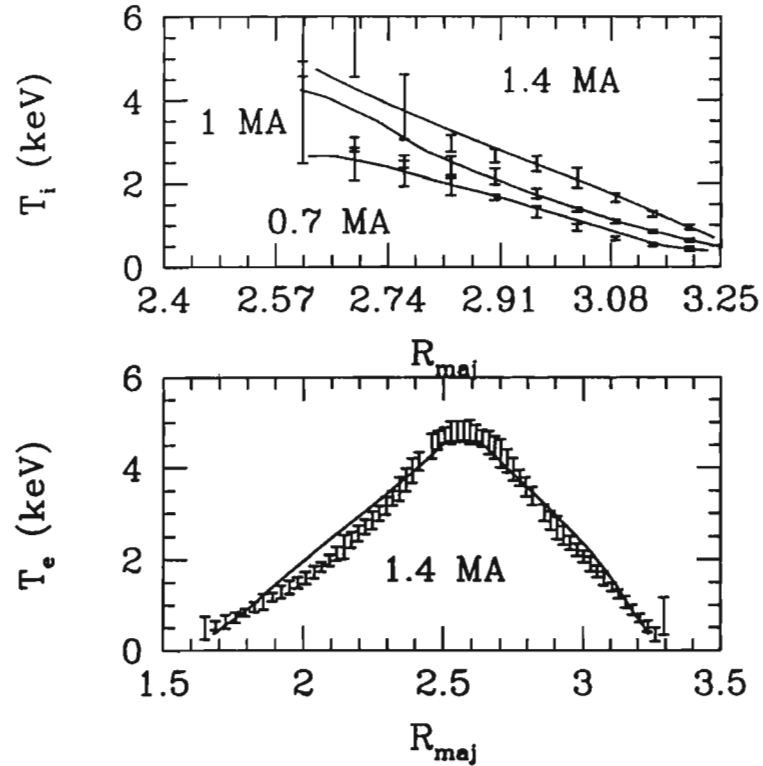
FIG. 2. TFTR current scan. The predicted quantities $T_i(r)$ and $T_e(r)$ compare well with experiment as the current is varied by a factor of two. Only one electron temperature profile is shown to increase legibility.

[With a quasilinear parameterization of the electron thermal diffusivity that was obtained from the gyrokinetic code ($\chi_e = 0.27\,\tau^{0.7}\chi_i$) we may also predict $T_e(r)$.]

The more complete power balance code runs as a post-processor to both SNAP and TRANSP, using measured or calculated values for $n_s(r)$, $q(r)$, $P_{rad}(r)$, beam deposition profiles, neoclassical conductivity, electron-ion equilibration, etc. Because the predicted thermal diffusivity is often too small in the edge region of the plasma, we use the experimentally determined temperature at $r/a \simeq 0.8$ as a boundary condition.

L mode Results

We have simulated more than 50 TFTR L-mode discharges (including the ρ^* scans) with reasonable success; the $T_i(r)$ [and $T_e(r)$] profiles are usually within $\pm 20\%$ of the experimental measurements. In Figs. (2) and (3) we show the predicted ion temperature profiles and the experimental measurements from current and power scans. We also show the predicted
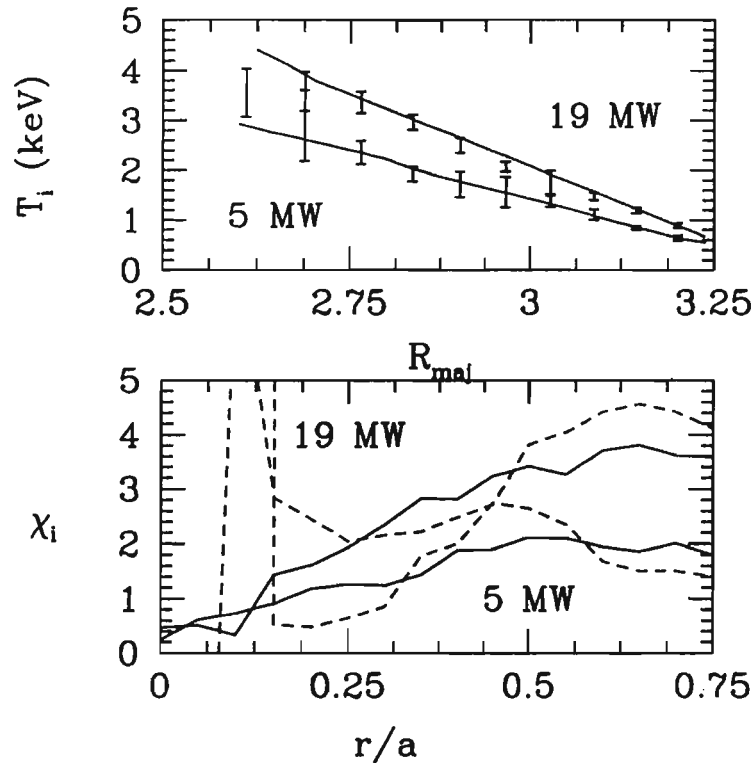
FIG. 3. TFTR power scan. The predicted $T_i(r)$ profiles agree reasonably well with the measured profiles as the power is varied by a factor of four. Moreover, the predicted values of χ_i increase robustly with minor radius.

and experimentally inferred $\chi_i(r)$, and a representative $T_e(r)$ profile. For $\chi_e \sim \chi_i$, $T_e(r)$ is determined primarily by electron-ion equilibration, obscuring possible errors in our estimate of χ_e. It is the increasing departure from marginality that overcomes the $T^{3/2}$ dependence of χ and leads to $\chi(r)$'s increase with minor radius. This result is a robust consequence of the form of χ.

Advanced Confinement Regimes

Our simulations are also consistent with several improved confinement regimes.

L mode/Supershot Transition

A puzzling aspect of TFTR supershots is the dependence of plasma performance on the recycling state of the limiter. Without addressing the edge conditions directly, simulations of low and high recycling discharges

TABLE I. LOW AND HIGH RECYCLING DISCHARGES

Shot	P_h(MW)	I_p(MA)	B_T(T)	$\bar{n}_e$	Exp. τ_E (ms)	Th. τ_E	Exp. $T_i(0)$	Th. $T_i(0)$
68719	19.3	2.0	4.8	5.8	87	84	4	4
68244	20.7	1.6	4.8	4.3	125	116	30	26
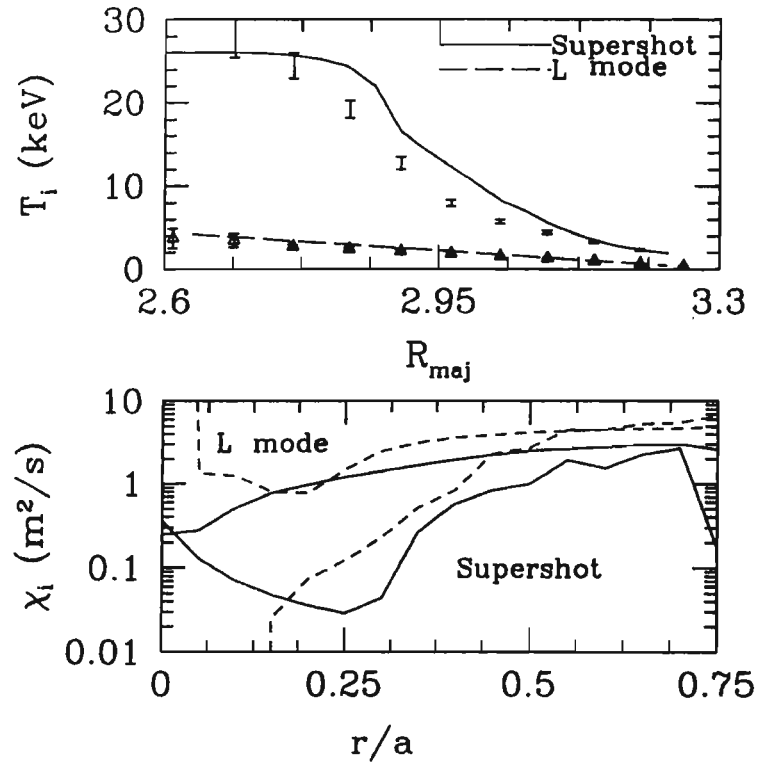
FIG. 4. TFTR L mode supershot comparison. The simulations capture much of the enormous variation in the ion temperature between supershots and L modes. Nonlinear simulations that include trapped electron dynamics will find a weaker critical gradient and will probably fit the data better.

that are otherwise very similar (see Table I) qualitatively recover the dramatic improvement in supershot performance. The simulations use the measured $T(r/a = 0.8)$ as a boundary condition. The simulation results are shown in Fig. (4); without nonlinear estimates of trapped electron mode contributions to the thermal diffusivity in the presence of sheared toroidal rotation, we expect and find that we over-estimate the stored energy somewhat. In the supershot simulation, χ_i increases by two orders of magnitude across the minor radius even though $T^{3/2}$ decreases by a factor of fifty. The improvement in performance in the supershot discharges we

have examined comes about from the complex dependences of $L_{T_i\text{crit}}$ on τ, R/L_n, the charge fraction of thermal deuterium (through n_b and Z_{eff}), and the edge boundary condition. The latter effects are amplified by the τ dependences of $\mathcal{F}$ and $L_{T_i\text{crit}}$. Some earlier analytic theories produced similar conclusions[9]. We have simulated more than twenty supershots with comparable success. The important conclusion is that the strong τ dependences are causal; high T_i/T_e improves the ion thermal confinement, regardless of how it arises.

While Eqs. (1) and (2) have utility, they nevertheless represent significant approximations to the fundamental simulations and consequently are the weakest component of this study. Within the simulation paradigm, it is a straightforward exercise to include additional physical effects. However, the extended parameter space one is led to consider is too large to map reliably; one is forced instead to consider individual scenarios.

Impurity Density Gradient Modes

We have not attempted to include the effects of impurity density gradient (IDG) modes in Eqs. (1) and (2), although their potential importance has long been known from local and sheared slab estimates[8]. Our gyrokinetic toroidal simulations confirm that impurity profiles more inwardly peaked than the electron profiles are stabilizing, and that more outwardly peaked impurity density gradients are strongly destabilizing.

Several experimental phenomena may be closely related to IDG modes. For example, our formulae produce thermal diffusivities that are often too small in the outer region of the plasma ($r/a > 0.85$). For typical parameters, however, ($Z_{\text{eff}} = 2.5$, *etc.*) toroidal simulations indicate that gradients as gentle as $L_{nC}/L_{ne} = -1$ can increase the growth rate of the ITG/IDG mode by a factor of 5. We thus confirm[8] that IDG modes are good candidates to explain the large χ_i near the edge. Quantitative experimental comparisons require a detailed description of the charge state distribution of carbon in the edge plasma. Pellet-injection experiments on TFTR[10] designed to test the marginality of plasmas to ITG modes are also strongly affected by inwardly peaked carbon gradients in the plasma core. The post-injection carbon gradient stabilization is quantitatively sufficient to bring the experimental results into agreement with the ITG results here.

VH mode Simulations

Eqs. (1) and (2) do not include the effect of velocity shear. We have, however, performed many toroidal nonlinear simulations including sheared flows with spatial equilibrium potentials[3] and with time-dependent ballooning transforms[5]. In the plasma core, where the plasma flow is almost purely toroidal, there is a stabilizing perpendicular shear rate, with $\gamma_{\perp} \equiv (r/q)\,d(V_{\phi}/R)/dr$ and a destabilizing parallel shear rate, such that $\gamma_{\parallel} \simeq (Rq/r)\gamma_{\perp}$. [Here, time is normalized by a/v_t]. Toroidal nonlinear simulations show that if $\gamma_{\perp}$ is comparable to the growth rate of the fastest-growing mode (including the parallel shear destabilization), ITG modes are stabilized[3]. Analysis of DIII-D VH mode discharges (with and without magnetic braking to control plasma rotation) with the linear gyrokinetic stability code[6] shows that $\gamma_{\perp} \sim \gamma_{\mathbf{max}}$ for cases in which the rotation has a demonstrable effect on the confinement. Finally, we find that for sufficiently high B_{θ}/B (or low Rq/r), the external torque on the plasma from the neutral beams can cause a bifurcation to appear, so that a steeper temperature gradient can be supported against the same power flow. This bifurcation may explain the H–VH transition.

PEP mode Simulations

Linear simulations show that ITG modes can be weakened or stabilized by relatively small levels of velocity shear if the magnetic shear is small. Substantially enhanced confinement in JET PEP modes is in good quantitative agreement with this stabilization mechanism. PEP mode discharges have a hollow or very flat q profile in the center so that the magnetic shear is small over a significant region ($r/a \leq 1/3$). Experimentally, the temperature gradient is found to increase strongly around the low shear region, indicating a substantial reduction in χ_i. The transition to this improved confinement region occurs over a short distance, $\Delta r/a \sim 0.05 - 0.1$. In this region, linear calculations indicate that diamagnetic levels of velocity shear can greatly weaken or stabilize ITG modes. The predicted location and sharpness of the transition regime agrees with experiment.

Preliminary nonlinear simulations confirm an enhancement (due to weak magnetic shear) of shear flow damping over the estimate described above, although the effect is weaker than linear simulations indicate. In these simulations, stabilization occurs for $\gamma_{\perp}/\gamma_{\mathrm{max}} \sim \min(0.5, \hat{s})$. Nonlinear simulations also indicate that reversed magnetic shear is intrinsically stabiliz-

ing for toroidal ITG modes. More work is needed to quantify the relative importance of these two stabilization mechanisms relevant to JET PEP mode discharges.

Conclusions

Comprehensive linear stability studies show that the ion temperature gradient is the dominant microinstability drive in TFTR L-mode plasmas; high-resolution nonlinear ITG simulations show that the associated thermal diffusivity is reasonably close to that inferred from experimental power balance calculations. Despite the strong decrease in temperature with minor radius, the predicted thermal diffusivities are found to increase robustly (for $r/a < 0.85$).

The existence of supershots (and hot-ion modes in general) may be understood from the parametric dependences of χ, especially T_i/T_e. Nonlinear simulations that include trapped electron modes and velocity shear will make this comparison more quantitative. The improved confinement observed in PEP modes and VH modes may be attributed to velocity-shear stabilization. In the former case, the stabilizing effects of the radial electric field are amplified by the weak magnetic shear. In the latter case, the observed toroidal rotation profile is sufficient to stabilize toroidal ITG modes that would otherwise be unstable. Finally, reversed magnetic shear may also play an intrinsic role in some advancement confinement regimes, as it has been found to be stabilizing in nonlinear simulations.

REFERENCES

[1] HAMMETT, G.W., PERKINS, F.W., Phys. Rev. Lett. **64** (1990) 3019.
[2] DORLAND, W., PhD Thesis, Princeton University, Princeton, NJ (1993).
[3] WALTZ, R.E., et al., Phys. Plasmas **1** (1994) 2229; also WALTZ, R.E., et al., Phys. Fluids B **4** (1992) 3138.
[4] BEER, M.A., PhD Thesis, Princeton University, Princeton, NJ (1994). The trapped electron models are also discussed in HAMMETT, G.W., et al., IAEA-CN-60/D-8, this volume.

[5]   WAELBROECK, F.L., CHEN, L., Phys. Fluids B **3** (1991) 601.

[6]   KOTSCHENREUTHER, M., et al., PPPL Rep. 2986, Princeton Plasma Physics Lab., Princeton, NJ (1994).

[7]   DONG, J.Q., et al., Phys. Fluids B **4** (1992) 1867.

[8]   COPPI, B., et al., Phys. Rev. Lett. **17** (1966) 377; also COPPI, B., et al., in Plasma Physics and Controlled Nuclear Fusion Research 1992 (Proc. 14th Int. Conf. Würzburg, 1992), Vol. 2, IAEA, Vienna (1993) 131.

[9]   ROMANELLI, F., BRIGUGLIO, S., Phys. Fluids B **2** (1990) 754.

[10] ZARNSTORFF, M.C., et al., in Plasma Physics and Controlled Nuclear Fusion Research 1990 (Proc. 13th Int. Conf. Washington, 1990), Vol. 1, IAEA, Vienna (1991) 109.

PLASMA PHYSICS AND CONTROLLED NUCLEAR FUSION RESEARCH 1994

PROCEEDINGS OF THE
FIFTEENTH INTERNATIONAL CONFERENCE ON PLASMA PHYSICS
AND CONTROLLED NUCLEAR FUSION RESEARCH
HELD BY THE
INTERNATIONAL ATOMIC ENERGY AGENCY
IN SEVILLE, 26 SEPTEMBER–1 OCTOBER 1994

In four volumes

VOLUME 3